Vaha-Savo, Lauri; Koivumaki, Pasi; Haneda, Katsuyuki; Icheln, Clemens; Chen, Jingjing

# 3-D Modeling of Human Hands for Characterizing Antenna Radiation from a 5G Mobile Phone

*Published in:*
2022 16th European Conference on Antennas and Propagation, EuCAP 2022

*DOI:*
10.23919/EuCAP53622.2022.9769053

Published: 01/01/2022

*Document Version*
Peer-reviewed accepted author manuscript, also known as Final accepted manuscript or Post-print

*Please cite the original version:*
Vaha-Savo, L., Koivumaki, P., Haneda, K., Icheln, C., & Chen, J. (2022). 3-D Modeling of Human Hands for Characterizing Antenna Radiation from a 5G Mobile Phone. In *2022 16th European Conference on Antennas and Propagation, EuCAP 2022* (Proceedings of the European Conference on Antennas and Propagation). IEEE. https://doi.org/10.23919/EuCAP53622.2022.9769053

# 3-D Modeling of Human Hands for Characterizing Antenna Radiation from a 5G Mobile Phone

Lauri Vähä-Savo*, Pasi Koivumäki*, Katsuyuki Haneda*, Clemens Icheln* Jingjing Chen†
*Aalto University School of Electrical Engineering, Espoo, Finland E-mail: lauri.vaha-savo@aalto.fi
†Huawei Technologies Sweden AB, Gothenburg, Sweden

***Abstract*—A method to obtain the three-dimensional (3D) model of a hand for an antenna-hand interaction analysis of a mobile phone is presented. The radiation and reception performance of millimeter-wave signals is more susceptible to intervention by a user's hand than that of legacy below-6 GHz radios. Hand models representing a wide range of natural handgrips of mobile phone users are therefore essential. The 3D modeling is based on the photogrammetry using a video footage of a hand. Multiple 3D models of natural handgrips can be obtained with reasonable efforts. The radiation performance of a canonical antenna array implemented into a mobile phone sized chassis is evaluated using a developed series of 3D hand models, showing the uncertainty of repeatable antenna-hand interaction analyses.**

***Index Terms*—mm-Waves, Mobile antenna evaluation, User hand effect.**

## I. Introduction

The successful deployment of millimeter-wave radios for the fifth-generation cellular mobile systems has been supported by careful design of radio hardware that mitigates the greater implementation losses at the band than legacy below-6 GHz bands. One of the significant implementation losses to be mitigated would be antenna-human interaction of a mobile phone. The interaction causes efficiency degradation due to absorption of the radiated power to human tissues and also due to changes of impedance matching conditions. Deformation of the radiation pattern is another apparent effect due to intervention of human hands. The former is classified into a near-field interaction, while the latter is characterized at the far-field. The detrimental effects of a human body on antenna radiation have been extensively studied for the legacy below-10 GHz bands, e.g., [1], [2], [3], [4], and references therein. For example, a thorough study of mobile phone grips has revealed its statistics [1] and their impacts on antenna radiation efficiency degradation [2]. When considering different hands, their variation in dielectric and conductive properties along with their grips affect the antenna radiation. The dielectric properties has been addressed in [3], [4] for 6-7 GHz band.

Recent studies pay more attention to millimeter-wave bands, e.g., [5], [6] and references therein. Because the size of antenna elements may be comparable to finger width, the positioning of antennas next to hands would make more drastic changes to their radiation characteristics than the lower frequency correspondents. Therefore it is important to perform *repeatable* evaluation of mobile phone antenna arrays. The repeatable evaluation is best feasible using phantoms in experiments and three-dimensional numerical models of hands in simulations. Focusing on simulations, a numerical model of a hand phantom specified by the Cellular Telecommunications Industry Association (CTIA) exists. It is also possible to obtain a hand grip using a three-dimensional (3D) modeling tool, e.g., Poser[1]. To the date, only a handful of 3D hand models are available for mobile antenna simulations. This paper therefore complements the lack of variations in the hand models through optical measurements of human hands with varying natural grips of a mobile phone. In particular, we use photogrammetry to generate realistic 3D simulation models from a large number of overlapping images. Photogrammetry-generated simulation models have found use in electromagnetic wave propagation simulations, e.g., ray-tracing [7]. The usefulness of the same for hand modeling is demonstrated in this paper, revealing the repeatability of millimeter-wave antenna simulations under the strong intervention of hands.

The rest of the paper is organized as follows: Section II introduces our photogrammetry modeling of human hands. Section III describes antenna radiation simulations using the obtained 3D hand models to reveal the extent of antenna simulation repetability. Section IV summarizes our work.

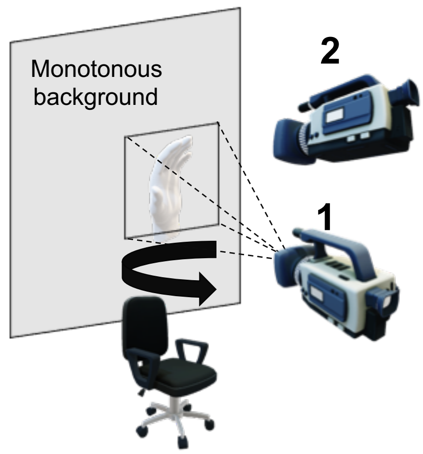


Fig. 1. Schematic of a photogrammetry measurement.

[1]https://www.posersoftware.com/

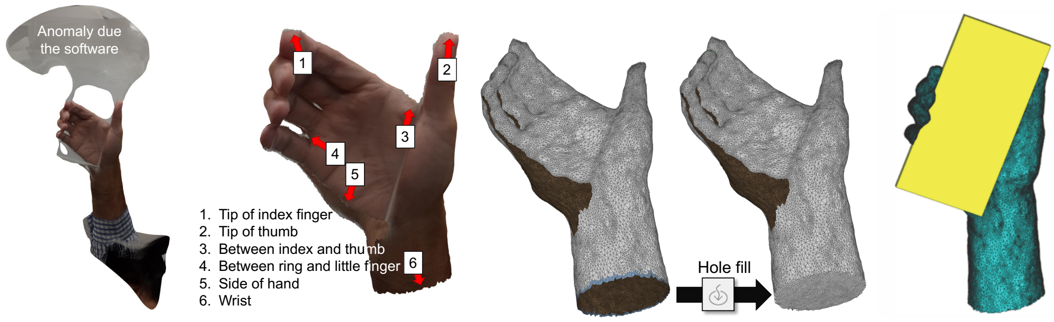


Fig. 2. Steps of photogrammetry modeling of a human hand: (a) a raw 3D model, (b) a rendered model with holes due to trimming an anomaly, (c) filling the holes and finally (d) the model imported to the *CST Studio Suite*; the yellow rectangle represents a phone chassis grasped by the hand.

## II. Photogrammetry of Human Hands

Photogrammetry requires multiple overlapping images of an object. To generate a complete model of the object, the images must cover the entire object. In this work, we film video footage of a hand and extract individual frames from the footage to be used as input images to a photogrammetry software, which is detailed in the following.

### A. Video Session Set Up

To set up the filming session easily and to eliminate background clutter, we maintain a stationary camera and rotate the hand instead. The hand is held against a monotonous background and rotated, achieving the same effect as if the camera was rotated around the hand. The experimental set up is illustrated in Fig. 1. Our experiments took place in a well-lit meeting room equipped with a large whiteboard. A test subject is seated on a swiveling office chair and holds their hand up, grasping a translucent piece of plexiglass. The plexiglass is cut to match the dimensions of a generic smart phone. This allows us to obtain images of the hand in a realistic grip pose while still seeing the palm of the hand through the plexiglass. The test subject is asked to grasp the plexiglass naturally as if they were holding a phone in their hand.

The test subject begins to rotate slowly on the swiveling chair while maintaining the grip of the plexiglass. A camera operator films the rotating hand such that approximately half of the test subject's forearm is always within the frame. While the rotation is happening, the camera operator makes slight adjustments to elevation of the camera to obtain footage of the hand from a range of elevation angles in addition to a full azimuth rotation.

In our experiments, the video footage was obtained using a 12 megapixel, 60 FPS camera. Typical sizes of the video file were approximately 90 Megabytes and duration approximately 70 seconds.

### B. Image Extraction

Images used as input of photogrammetry are obtained from individual frames of the video footage. A number of different programs are capable of achieving this. In this work, we use the software *VLC Media Player*[2] and its Scene Filter functionality. A total of 100 individual images are extracted from the video at even intervals of time frames. The images fully cover the hand from a range of azimuth and elevation angles.

### C. Hand Model Generation and Processing

The 100 images are processed using *Autodesk ReCap Photo*[3]. The result is a 3D model of a human hand grasping a translucent object with a realistic grip. An example of the raw 3D model is shown in Fig. 2a. We can note the following features. A section of the subject's head is present in the model, seen as a dark mass in its lower part. Edges of the plexiglass are seen in the mode as well, as its sides were not as translucent as rest of the piece. Finally, an anomaly can be seen above the model in the form of a grey blob due to the software recognizing reflections of the room light on the background whiteboard.

A set of steps must be taken to refine the raw 3D model for antenna simulations. First, excess parts of the model must be cut away. A range of software are capable of manipulating 3D models for the purpose; we used the software *CloudCompare*[4], resulting in the model in Fig. 2b where different sections of the hand were cut. It is necessary for the model to be a closed surface such that it is usable for antenna simulations. A range of software and algorithms exist to close holes in 3D meshes, and in this work we chose to use built-in functionality `Hole fill` of *Autodesk ReCap Photo*. This step is illustrated in Fig. 2c, where the hole left from removing the forearm is filled. After the model has been sufficiently cleaned and resulting holes closed, it can be imported to electromagnetic field solvers, e.g., *CST Studio Suite*[5], for hand-antenna interaction simulations. The final model is shown in Fig. 2d, where a model of the phone chassis is placed in the hand.

The hands of three people, measured twice for their natural hand grips, led to 6 hand models using our 3D modeling method. Between filming two videos of the same user's hand

[2]https://www.videolan.org/vlc/
[3]https://www.autodesk.com/
[4]https://www.danielgm.net/cc/
[5]https://www.3ds.com/products-services/simulia/products/cst-studio-suite/

for different natural grips, the Plexi model of the phone was released and similar hand grip was taken again.

## III. Antenna-Hand Interaction

### A. 28 GHz Antenna Array

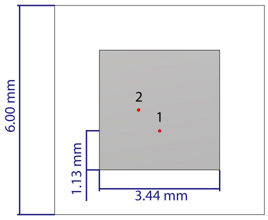


(a)

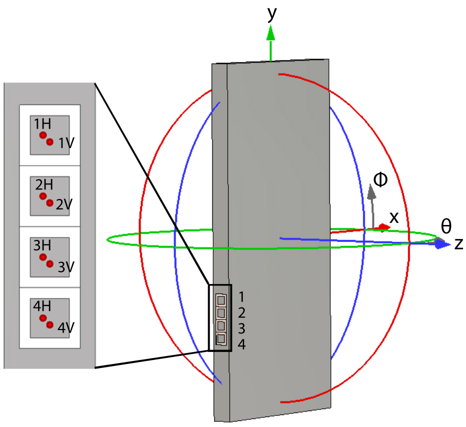


(b)

Fig. 3. (a) Dimensions of dual-polarized antenna element, (b) Antenna array in the mobile phone chassis with the element numbers and coordinate system. The gray areas are metal and white areas are the PCB substrate.

Our choice for antenna element to use in a mobile phone chassis is a dual-polarized patch antenna element resonating at 28 GHz, presented in [8]. The element is realized on 0.107 mm thick Rogers 5880 substrate with relative permittivity of 2.2 and metal thickness of 17 $\mu$m. The feeds are realized with discrete ports in *CST Studio Suite*. The ideal feed structure minimizes the mismatch loss and ensures high radiation efficiency in free space. Element dimensions are shown in Fig. 3a. Four of these elements are used to form 4-element linear array on one of the long side of $150 \times 75$ mm sized phone chassis. The center of the array is located at 37.5 mm from the bottom of the phone chassis. The location of the array in the chassis, element numbering and a definition of the spherical coordinate system is shown in Fig. 3b. The two feeds of a single antenna element radiate mainly horizontal- (H-) and vertical- (V-) polarizations according to the spherical coordinate system. The antenna and array designs are canonical ones on a mobile phone sized chassis, and do not represent actual implementation of them in any commercial products.

### B. Antenna Radiation

The six 3D hand models introduced in Section II are combined with the mobile phone chassis including the linear array. The photogrammetry-based hand-model generation is limited to producing the hand shape as a mesh, but it does not provide the correct dimensions of the hand. Therefore, when importing the hand model into CST, we need to rescale the 3-D mesh with help of the visible imprints of the plexiglass in the hand palm. Then, the phone chassis is placed in each hand fitting as well as possible into these imprints. The chassis is placed in each hand so that its location is similar to the actual grip during the photogrammetry measurement. Figure 4 shows the side view of the handgrips with the mobile phone chassis in the simulations. In the first handgrip (Fig. 4a, named "Hand 1" hereinafter), the first element is partly covered and the fourth element is fully covered by the fingers. In the second handgrip (Fig. 4c named "Hand 2"), antenna elements other than the first one are covered by the fingers. In the case of the third handgrip, all the elements are covered by the hand (Fig. 4e as "Hand 3"). The second natural grip of the same hand have some differences compared to the first ones. For example in case of the Hand 1 (see Figs. 4a and 4b), in the first grip the first element was only partly covered by the finger but in the the second grip it is fully covered by the finger. It is clearly demonstrated that the natural grips of mobile phone users make significantly different covering of a possible antenna array design on a chassis. Also we can see small differences between two different grips of the same person's hand which may affect significantly the radiation of

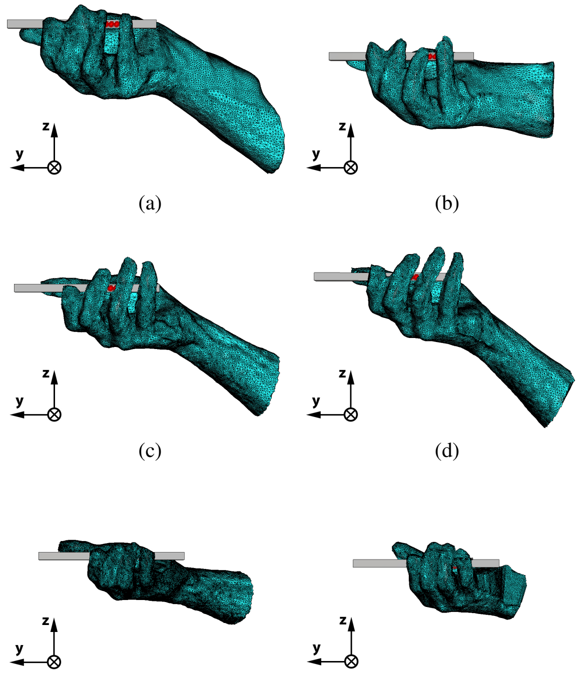

(a) (b) (c) (d) (e) (f)

Fig. 4. Three different hands with two natural grips of a mobile phone sized chassis (left and right are grips 1 and 2 by the same person, respectively). The six resulting 3-D mesh models a)-f) are used in simulations with a mobile phone chassis including a linear antenna array. Visible red dots indicate array elements that are not covered.

the antenna array.

The permittivity of the hand in the simulations is set to be the same as the human skin ($\epsilon_r = 16.55$ and $\sigma = 25.82$ S/m) at 28 GHz [9]. The hand is assumed to be homogeneous in terms of its permittivity. Since the penetration depth of human skin is roughly 1 mm at 28 GHz and the thickness of human skin varies between 1.3 and 2.9 mm [10], accurate anatomical modeling of hands deeper than the skin is not necessary. Radiated fields from all eight antenna feeds are solved using the time-domain simulator in the *CST studio Suite*, followed by beamforming performed in post-processing using the *Matlab*. We consider the realized gain, i.e., the antenna gain including the mismatch losses, of a broadside beam of the linear array, i.e., to $-x$ direction. The same beamforming weights are applied separately to a set of V- and H-polarized feeds of the array, resulting in two synthesized beams for two orthogonal polarizations according to the spherical coordinate system defined in Fig. 4. The same weights are used in both free space and hand simulations.

TABLE I
PEAK REALIZED GAINS OF THE BROADSIDE BEAMS

| Grip | Pol. | Free space | Hand 1 | Hand 2 | Hand 3 |
|---|---|---|---|---|---|
| 1 | V | 12.1 dBi | 7.1 dBi | 0.4 dBi | −11.1 dBi |
| 1 | H | 12.3 dBi | 6.9 dBi | 2.6 dBi | −4.8 dBi |
| 2 | V | 12.1 dBi | 4.0 dBi | −3.0 dBi | −9.0 dBi |
| 2 | H | 12.3 dBi | 4.2 dBi | −2.1 dBi | −1.8 dBi |

TABLE II
RADIATION EFFICIENCIES OF THE LINEAR ANTENNA ARRAY

| Grip | Pol. | Free space | Hand 1 | Hand 2 | Hand 3 |
|---|---|---|---|---|---|
| 1 | V | 0.94 | 0.54 | 0.21 | 0.02 |
| 1 | H | 0.96 | 0.63 | 0.21 | 0.04 |
| 2 | V | 0.94 | 0.41 | 0.06 | 0.02 |
| 2 | H | 0.96 | 0.40 | 0.07 | 0.03 |

Figure 5 shows $xy$ and $xz$ cuts of the broadside beams for the H- and V-polarized synthesized beams; see coordinate system from Fig. 4. Tables I and II summarize maximum realized gains of the synthesized beams and radiation efficiencies, demonstrating that radiation properties of the canonical array is drastically affected by natural handgrips of the three mobile users. The radiation efficiencies, on Table II, tells us that the hands mainly absorbs the radiation. Some RF friendly clearance material between antennas and hand might help us to get better efficiency for our array. Table I also clearly shows lower realized gain as more elements are blocked. It is interesting to note that the V-polarized beam is affected more than H-polarized beam for Hands 2 and 3. This might be caused by the fact that the sides of the patch antenna element that are facing in $\pm z$ directions are the ones that have higher current distribution when we are feeding V-polarized feeds. The first part of the antenna that fingers tough is the side that faces $-z$ direction which will disrupt the current distribution and affects the V-polarized beam more than the H-polarized beam.

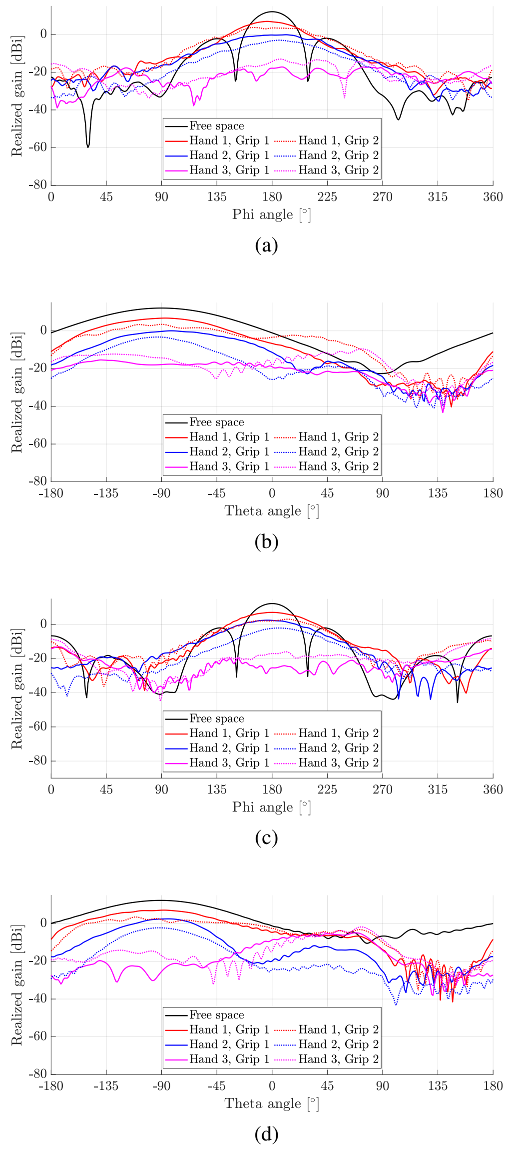


Fig. 5. a) $xy$ plane cut of the synthesized broadside beam for V-polarization and b) $xz$ cut of the same; c) $xy$ cut of the synthesized broadside beam for H-polarization and d) $xz$ cut of the same.

## C. Impacts of Hand Modeling Repeatability

Finally, we created a new realization of Hand 3 model from the same video that produced the "grip 1" model. Depending on a set of images extracted from the same video footage, it is possible to end up with different 3D models of the same handgrip, thereby repeatability of our modeling method may be affected. We call the new realization of the "grip 1" model as "grip 1 repeat" hereinafter. The peak realized gain of broadside beam was $-9.1$ and $-7.1$ dBi, for V- and H-polarizations respectively. The peak gain differs up to 2.3 dB between the "grip 1" and "grip 1 repeat". The radiation efficiency of V-polarization is lower in the simulation with "grip 1 repeat" by 0.003 and for H-polarization efficiencies are the same between the two models. This means that the hand directs radiation differently in our two simulations. There are a few reasons that could explain this small difference. First, due to limitations of the photogrammetry method, we need to manually rescale the hand-mesh in CST as discussed above. This causes some uncertainty in the final hand dimensions of the CST-model. Another source of difference is the placement of the antenna array in hand grips, which were implemented manually. Alignments of the chassis in different hand grips are somewhat arbitrary, even though the hand models come from the same person. It turned out from our simulations that small variations in distance between the hand and the array caused the observed differences in radiation performances. They are the uncertainty of the repeatable tests of antenna radiation simulations under the presence of a user's hand.

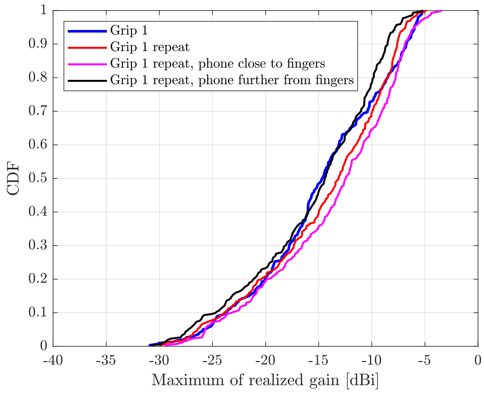


Fig. 6. Statistics of the spherical coverage with different realizations of "Hand 3" and placements of the mobile phone chassis in the models.

To characterize the uncertainty more in detail, the spherical coverage of the antenna array held by the two models of Hand 3, grip 1, was evaluated. The spherical coverage was calculated the same way as shown in [6]. We perform beam scanning in a post data-processing of individual radiation patterns of antenna feeds where a 3-bit phase shifter is assumed at all eight ports. This way we will end up with 1024 beams, from which we find the maximum gain at each direction. Statistics of the spherical coverage are analyzed using the cumulative distribution function (CDF). We used three realizations of the same person's specific grip, while varying the phone location slightly over $\pm 0.5$ mm in the $x$-direction. The simulation reveals the effect of small displacement of the mobile phone chassis to the spherical coverage. The CDF shown in Fig. 6 shows that curves are slightly different. The "grip 1" and "grip 1 repeat" of Hand 3 have a mean absolute difference of $0.75$ dB. A small variation of the mobile phone location causes a maximum difference of 2.5 dB at a specific cumulative level, indicating the level of uncertainty that we have to expect in repeatable simulations.

## IV. Concluding Remarks

In order to complement the lack of variation in 3D models of handgrips for antenna-hand interaction analyses, this paper introduced a convenient handgrip modeling method based on the photogrammetry. Obtaining a single 3D model of an actual handgrip requires half-a-day efforts, including importing them to an electromagnetic field solver. This paper considered hands of three particular persons and a reference antenna array. Their effects on mobile antenna radiation are not comparable with those reported in other literature where different hand models and arrays were considered. The 3D models allow repeatable analyses of antenna-hand interaction, provided that it is possible to place the model of a mobile phone chassis precisely in the hand model. In our manual placement of the chassis into the obtained hand models, the uncertainty was up to 2 dB in far-field gains and 2.5 dB in statistics of the spherical coverage at a specific cumulative level. Antenna-hand interaction analyses at millimeter-waves are on-going to find a robust geometry of a mobile phone antenna array while considering natural handgrips of many different users. As a future work, to be able to confirm the efficiency of the presented method we are going to compare presented simulation method to measurements with multiple users and handgrips, including right, left and double handed grip.

## Acknowledgement

The authors would like to acknowledge discussion opportunities with experts in Huawei Technologies Sweden AB and Huawei China.

## References


[1] M. Pelosi, O. Franek, M. B. Knudsen, M. Christensen, and G. F. Pedersen, "A grip study for talk and data modes in mobile phones," *IEEE Trans. Ant. Prop.*, vol. 57, no. 4, pp. 856–865, 2009.

[2] M. Pelosi, O. Franek, M. B. Knudsen, G. F. Pedersen, and J. B. Andersen, "Antenna proximity effects for talk and data modes in mobile phones," *IEEE Ant. Prop. Mag.*, vol. 52, no. 3, pp. 15–27, 2010.

[3] S. S. Zhekov, O. Franek, and G. F. Pedersen, "Dielectric properties of human hand tissue for handheld devices testing," *IEEE Access*, vol. 7, pp. 61 949–61 959, 2019.

[4] S. S. Zhekov and G. F. Pedersen, "Effect of dielectric properties of human hand tissue on mobile terminal antenna performance," in *Proc. 14th European Conf. Ant. Prop. (EuCAP 2020)*, Copenhagen, Denmark, 2020, pp. 1–5.

[5] K. Zhao, Z. Ying, S. Zhang, and G. Pedersen, "User body effects on mobile antennas and wireless systems of 5G communication," in *Proc. 14th European Conf. Ant. Prop. (EuCAP 2020)*, Copenhagen, Denmark, 2020, pp. 1–5.

[6] L. Vähä-Savo, C. Cziezerski, M. Heino, K. Haneda, C. Icheln, A. Hazmi, and R. Tian, "Empirical evaluation of a 28 GHz antenna array on a 5G mobile phone using a body phantom," *IEEE Trans. Ant. Prop.*, 2021.

[7] V. Semkin, D. Solomitckii, R. Naderpour, S. Andreev, Y. Koucheryavy, and A. V. Räisänen, "Characterization of radio links at 60 GHz using simple geometrical and highly accurate 3-D models," *IEEE Trans. Veh. Tech.*, vol. 66, no. 6, pp. 4647–4656, June 2017.

[8] M. Heino, C. Icheln, and K. Haneda, "Self-user shadowing effects of millimeter-wave mobile phone antennas in a browsing mode," in *Proc. 13th European Conf. Ant. Prop. (EuCAP 2019)*, Krakow, Poland, Apr. 2019, pp. 1–5.

[9] S. Gabriel, R. Lau, and C. Gabriel, "The dielectric properties of biological tissues: III. parametric models for the dielectric spectrum of tissues," *Physics in medi. biol.*, vol. 41, pp. 2271–93, Dec. 1996.

[10] T. Wu, T. S. Rappaport, and C. M. Collins, "Safe for generations to come: considerations of safety for millimeter waves in wireless communications," *IEEE Microw. Mag.*, vol. 16, no. 2, pp. 65–84, Mar. 2015.